Available online at www.sciencedirect.com
ScienceDirect
Journal of the Mechanics and Physics of Solids
54 (2006) 2592–2620

JOURNAL OF THE MECHANICS AND PHYSICS OF SOLIDS

www.elsevier.com/locate/jmps

Brain tissue deforms similarly to filled elastomers and follows consolidation theory

G. Franceschini[a], D. Bigoni[a,*], P. Regitnig[b], G.A. Holzapfel[c]

[a]*Dipartimento di Ingegneria Meccanica e Strutturale, Università di Trento, Via Mesiano 77 – 38050 Povo, Trento, Italia*
[b]*Institute of Pathology, Medical University of Graz, Auenbruggerplatz 25, A-8036 Graz, Austria*
[c]*School of Engineering Sciences, Royal Institute of Technology, Osquars backe 1, SE-100 44 Stockholm, Sweden, and Computational Biomechanics, Graz University of Technology, Schiesstattgasse 14-B, A-8010 Graz, Austria*

Received 20 October 2005; received in revised form 2 May 2006; accepted 3 May 2006

Abstract

Slow, large deformations of human brain tissue—accompanying cranial vault deformation induced by positional plagiocephaly, occurring during hydrocephalus, and in the convolutional development—has surprisingly received scarce mechanical investigation. Since the effects of these deformations may be important, we performed a systematic series of in vitro experiments on human brain tissue, revealing the following features. (i) Under uniaxial (quasi-static), cyclic loading, brain tissue exhibits a peculiar nonlinear mechanical behaviour, exhibiting hysteresis, Mullins effect and residual strain, qualitatively similar to that observed in filled elastomers. As a consequence, the loading and unloading uniaxial curves have been found to follow the Ogden nonlinear elastic theory of rubber (and its variants to include Mullins effect and permanent strain). (ii) Loaded up to failure, the "shape" of the stress/strain curve qualitatively changes, evidencing softening related to local failure. (iii) Uniaxial (quasi-static) strain experiments under controlled drainage conditions provide the first *direct* evidence that the tissue obeys consolidation theory involving fluid migration, with properties similar to fine soils, but having much smaller volumetric compressibility. (iv) Our experimental findings also support the existence of a viscous component of the solid phase deformation.

*Corresponding author.
E-mail addresses: giulia.franceschini@ing.unitn.it (G. Franceschini), bigoni@ing.unitn.it (D. Bigoni), peter.regitnig@meduni-graz.at (P. Regitnig), gh@biomech.tu-graz.ac.at (G.A. Holzapfel).

0022-5096/$ - see front matter
doi:10.1016/j.jmps.2006.05.004

Brain tissue should, therefore, be modelled as a porous, fluid-saturated, nonlinear solid with very small volumetric (drained) compressibility.

Keywords: Soft tissue; Biphasic material; Human brain; Elasticity; Terzaghi consolidation

1. Introduction

Intentional cranial deformation by manipulation or constraining apparatuses is an archaic cultural practice adopted by various ethnic groups at different times in every continent (Dingwall, 1931). Similar, though unintentional, creeping deformations arise in forms of brachycephaly and plagiocephaly that may be developed by supine-sleeping infants and corrected by helmet therapy (Hutchison et al., 2004). During these processes, brain tissue slowly deforms following movements of the cranial vault. Large and sometimes huge quasi-static deformations of the brain tissue may occur during hydrocephalus (Lewin, 1980). Does the brain tissue undergo *damage* during these deformations? Is the deformation influenced by the presence of *interstitial fluids*? Consolidation of porous fluid-saturated material is known to involve "delayed" effects taking place over a long time scale—a famous example borrowed from geotechnical engineering is the continuous moving of the Pisa tower through eight centuries, consequent to consolidation of fluid-saturated clayey soil in the underlying ground (Burland et al., 2003)—so, are the effects of consolidation important for brain tissue?

The answer to these questions is related to the knowledge of mechanical properties of brain parenchyma under quasi-static tests at large deformations and under conditions of controlled drainage. The same mechanical properties are crucial in analysing normal and pathological convolutional development. Therefore, tensile/compressive tests are essential to validate mechanical based theories (Richman et al., 1975; Van Essen, 1997), which explain folding of the brain structure without recurring to mechanical interaction with the cranial vault [a fact consistent with findings by Kingsbury et al. (2003)].[1] In these theories interstitial fluid—although believed of fundamental relevance in different situations involving brain deformation, for instance hydrocephalus (Hakim et al., 1976)—does not play a role. We will see that this can be justified on the basis of the results that will be presented.

Motivated mainly by the modelling of traumatic brain injury, which often occurs under dynamic conditions, efforts have been made to measure the mechanical properties of brain tissue, starting from the pioneering works by Fallenstein et al. (1969) and Galford and McElhaney (1969), but the situation remains rather unsatisfactory, see Appendix A for a review. In particular, it is a matter of debate whether brain tissue should be regarded as a highly viscous gel or as a solid or as a fluid-saturated solid; if it is a compressible material or if it is only capable of isochoric deformation; if it can be modelled using the linear or the nonlinear theory of elasticity with or without anisotropy; if it exhibits viscoelastic behaviour or if it exhibits permanent deformations. Mechanical simulations have been performed by employing each of the above-mentioned model assumptions, see, for

[1]The tension-based theory by Van Essen has received additional support from Scannell (1997); the theory itself stimulates the need of mechanical experiments on brain tissue for further progress.

example, the recent review by Kyriacou et al. (2002). Moreover, the quasi-static behaviour up to failure did not receive substantial attention and the role of interstitial fluid, although believed to be important, has never been experimentally discriminated from other factors possibly playing similar roles, such as viscosity.

The present article is organized as follows. Uniaxial stress, cyclic tension/compression experiments are presented in Section 2; the main result is that the material is shown to behave qualitatively similar to filled elastomers and is, therefore, shown to follow the Ogden (1972) constitutive theory [and subsequent modifications in terms of the so-called "pseudo-elasticity" theory, to include Mullins effect (Ogden and Roxburgh, 1999) and permanent deformations (Dorfmann and Ogden, 2004)] for rubber. However, damage until failure is also investigated, evidencing a kind of fracture typical of fibrous material. Uniaxial strain experiments at free drainage at the top and bottom of a sample are presented in Section 3. These provide the first direct experimental evidence that brain tissue follows consolidation theory for biphasic materials. Although our results clearly indicate that consolidation is the leading mechanism under quasi-static uniaxial strain, we show that adding a viscous term to the solid phase yields an almost complete adherence between experimental results and the biphasic theory. Therefore, our results not only do not exclude, but rather support a viscous behaviour of the tissue.

2. Uniaxial cyclic tension/compression experiments

In order to answer the above mentioned issues, and to lay the foundation for a physically motivated mechanical model for slow and large deformations of brain tissues, we have performed a systematic series of in vitro experiments on human tissue excised during autopsy within 12 h of death (use of autopsy material from human subjects was approved by the Ethics Committee, Medical University of Graz, Austria).

Uniaxial, quasi-static cyclic tension/compression experiments at a speed of 5 mm/min (corresponding to initial strain rates ranging between 5.5 and $9.3 \times 10^{-3}\,s^{-1}$) were performed on 86 cylindrical and prismatic specimens taken at different orientations and different locations within the brain (see Appendix B for details). For the first time, loading cycles have been performed at various load levels until large strain, damage and final failure of the specimen have been reached. Results have been found to be qualitatively similar for all samples, with a typical nominal stress versus uniaxial stretch response such as that shown in Fig. 1, from two tests on white matter, one involving compression and subsequent tension (left) and another involving tension and subsequent compression (right). Both tests were performed up to a stretch level still far from failure, but near damage initiation. The behaviour evidences: strong nonlinearity;[2] hysteresis; different stiffnesses in tension and compression, and during loading and unloading [analogous to the so-called "Mullins effect" in elastomers (Mullins, 1947)]; permanent deformations (also observed by Hakim and co-workers, who called them "bio-plastic", Hakim et al., 1976).

[2]The initial curvature of the curve (convex downward, so called "S-shaped") in the tension/compression experiment, observed for the first time on human brain by Miller and Chinzei (2002), represents another feature distinguishing brain parenchyma from other soft tissues (for instance biological gels, Storm et al., 2005), but common to materials characterized by chain-like particles, including: rubber, cellulose, wool, and paint films (Hourwink, 1958) and DNA molecules (Cluzel et al., 1996).

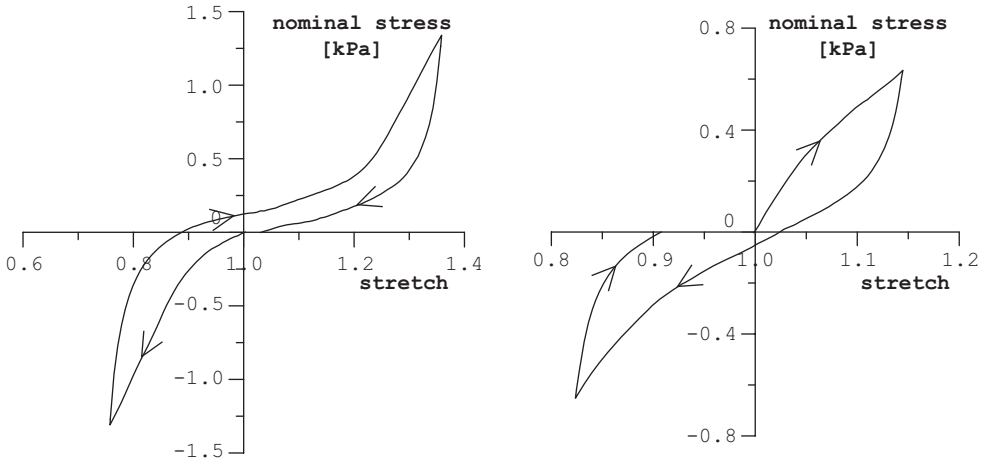

Fig. 1. Representative results of compression/tension (left) and tension/compression (right) tests to a stretch well below fracture but approaching the damage threshold on [14 mm/9.5 mm (left) and 14 mm/9 mm (right) initial height/edge] prismatic specimens of white matter, harvested from the occipital lobe (left) and from the frontal lobe (right), in the frontal direction. Nominal stress is reported versus stretch. Arrows indicate the loading direction.

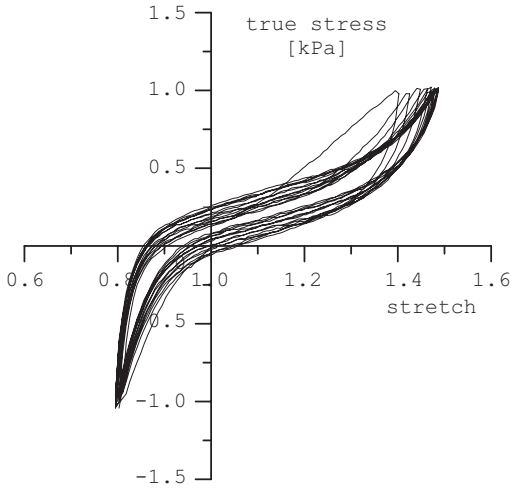

Fig. 2. Effect of cyclic loading in a compression/tension test. Nominal stress vs. stretch representation shows preconditioning in a (11 mm/7 mm initial height/edge) prismatic specimen of white matter harvested from the parietal lobe in the frontal direction.

Preconditioning was also observed, as indicated in Fig. 2, from a sample harvested from the parietal lobe in the frontal direction and subject to 14 compression/tension cycles.

It is important now to mention that (as will become apparent later), due to the fact that the volumetric drained deformability will be found to be very small, the above-described experimental results are believed to be only marginally affected by the bi-phasic nature of

the material (so that there is no need here to distinguish between drained and undrained behaviour for uniaxial tension/compression tests).

Qualitatively, the stress–strain behaviour is very similar to that of filled elastomers (Lion, 1997). It, therefore, appears natural to compare with the Ogden (1972, 1986) theory of nonlinear, incompressible elasticity for rubberlike materials. Within this framework, the nominal uniaxial stress t is related (due to incompressibility) to the longitudinal stretch λ through

$$t = \sum_{i=1}^{N} \mu_i(\lambda^{\alpha_i - 1} - \lambda^{-0.5\alpha_i - 1}), \tag{1}$$

where μ_i and α_i are constitutive parameters.

The comparison between our experimental data and the constitutive Eq. (1) turns out to be particularly satisfactory, except that Ogden's theory neither accounts for any permanent deformation, nor describes the Mullins effect. However, Eq. (1) has been found to describe with great accuracy all loading and unloading curves taken separately, when shifted to the origin of axes, with only two terms μ_1, μ_2 and corresponding α_1, α_2. In particular, the following values of the above parameters have been found[3]: $\mu_1 = 1.044$ (mean value; range: $-10.8 \div 23.5$; standard deviation: 7.722) kPa, $\mu_2 = 1.183$ (mean value; range: $-4.0 \div 19.7$; standard deviation: 5.942) kPa, $\alpha_1 = 4.309$ (mean value; range: $-22.0 \div 29.5$; standard deviation: 17.892) and $\alpha_2 = 7.736$ (mean value; range: $-18.3 \div 50.9$; standard deviation: 21.967) (Franceschini, 2006). It is important to note that the products $\mu_1\alpha_1$ and $\mu_2\alpha_2$ have been always found positive in our identifications, in particular, $\mu_1\alpha_1 = 1.244$ (mean value; range: $0.00026 \div 3.240$; standard deviation: 1.315) kPa and $\mu_2\alpha_2 = 0.822$ (mean value; range: $0.038 \div 2.381$; standard deviation: 0.767) kPa.

Other authors (Miller and Chinzei, 1997, 2002; Prange and Margulies, 2002) have also successfully employed elasticity models (augmented with viscosity) for describing the loading response of the material, however, the fact that the Ogden model fits not only the loading, *but also the unloading curves* separately is a clear indication that a modelling of the brain tissue can be pursued by employing pseudo-elasticity (which essentially means combining different "elastic" responses for loading and unloading, see Ogden and Roxburgh, 1999). This approach has never previously attempted, but turns out to be satisfactory. In particular, using the model for the Mullins effect (but not for permanent deformation) proposed by Ogden and Roxburgh (1999), the material response can be described in terms of a pseudo energy-function (for uniaxial stress)

$$W(\lambda, \eta) = \eta W(\lambda) + \phi(\eta), \tag{2}$$

where $W(\lambda)$ is the strain energy corresponding to the Ogden model

$$W(\lambda) = \sum_{i=1}^{N} \mu_i(\lambda^{\alpha_i} + 2\lambda^{-\alpha_i/2} - 3)/\alpha_i, \tag{3}$$

[3]The above parameters have been obtained imposing that model (1) predicts the same tangent at the origin and the same initial and final points of the experimental curve, with a given value of α_1. The value of α_1 has been selected by a trial-and-error procedure. Although very simple and efficient, our identification procedure does not a-priori guarantee that the product $\mu_i\alpha_i$ (index not summed) is positive (in which case the material response would not be a-priori stable, Ogden, 1972). An alternative (more complicated) identification technique in which positiveness of $\mu_i\alpha_i$ is ensured was provided by Twizell and Ogden (1983).

so that the nominal stress turns out to be that given by Eq. (1), but multiplied by η, the following function of the current stretch:

$$\eta = 1 - \frac{1}{r}\mathrm{erf}\left[\frac{1}{m}(W(\lambda_m) - W(\lambda))\right], \tag{4}$$

in which r and m are material parameters and λ_m represents the stretch at which unloading initiates. Therefore, along the primary loading path, η is hold constant and equal to unity, whereas parameter η begins decreasing starting from $\lambda = \lambda_m$, to account for the stress softening during unloading. Except that permanent deformations are not captured, we have found a good agreement of our data with the above model, as shown in Fig. 3, where two specimens of white matter have been considered.

The residual strain upon unloading can be accounted for by employing the Dorfmann and Ogden (2004) model for rubber materials. They introduced a pseudo strain-energy function depending on two parameters, η_1 and η_2. The former is associated to the Mullins effect (thus playing the role of η in the Ogden and Roxburgh model), the latter to the permanent strain. The nominal stress (in an uniaxial state) results

$$t = \eta_1 W(\lambda) + (1 - \eta_2)(v_1\lambda - \bar{v}_2\lambda^{-2}), \tag{5}$$

where

$$\eta_1 = 1 - \frac{1}{r}\tanh\left[\frac{W(\lambda_\mathrm{m}) - W(\lambda)}{m\mu}\right], \quad \eta_2 = \frac{1}{r}\tanh\left[\left(\frac{W(\lambda)}{W(\lambda_\mathrm{m})}\right)^{\alpha[W(\lambda_\mathrm{m})]}\right] / \tanh(1), \tag{6}$$

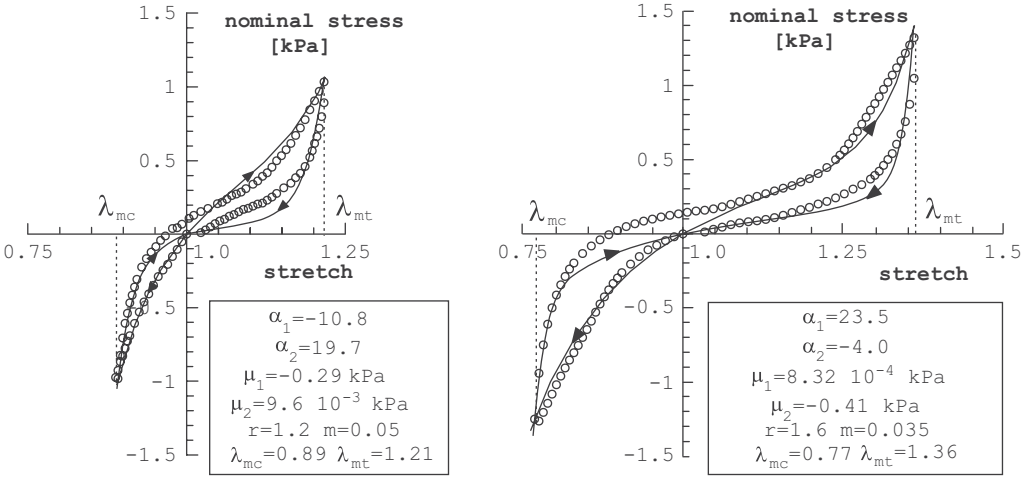

Fig. 3. Comparison between the experimental data for two compression/tension tests and Ogden and Roxburgh (1999) model for Mullins effect. Cylindrical specimens of white matter (10 mm/8 mm initial height/diameter, left) harvested from frontal lobe in the sagittal direction and prismatic specimen of white matter (14 mm/9.5 mm initial height/edge, right) harvested from occipital lobe in the frontal direction have been used.

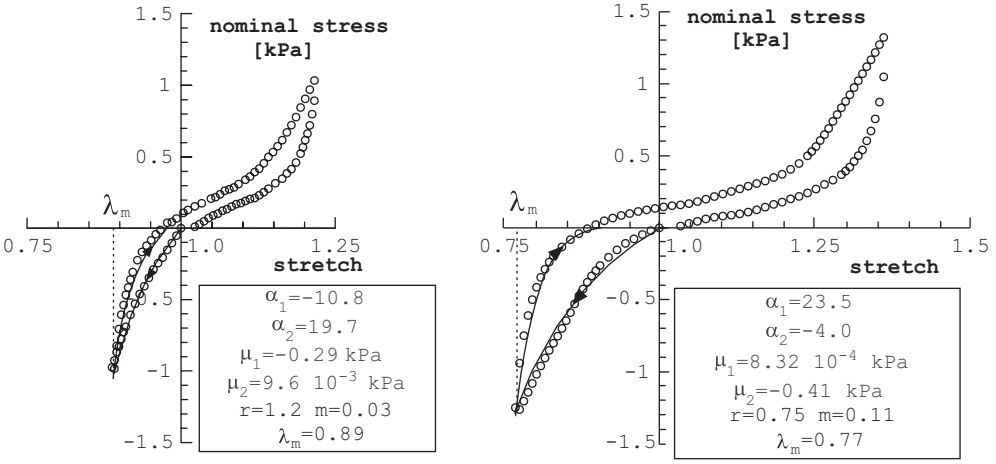

Fig. 4. Comparison between the experimental data for two compression/tension test and Dorfmann and Ogden (2004) model for Mullins effect and permanent deformation. The experimental data are the same used in Fig. 3.

$$v_1 = 0.4\mu\left[1 - \frac{1}{3.5}\tanh\left(\frac{\lambda_m - 1}{0.1}\right)\right], \quad \bar{v}_2 = 0.4\mu, \tag{7}$$

and

$$\alpha[W(\lambda_m)] = 0.3 + 0.16\frac{W(\lambda_m)}{\mu}, \quad \mu = \frac{1}{2}\sum_{i=1}^{N}\mu_i\alpha_i. \tag{8}$$

The above model correctly fits the unloading response from compression or tension (see Fig. 4, referred to the same specimens considered in Fig. 3). However, the model has been found to be completely inadequate to describe the transition between tension and compression (and viceversa), which has therefore omitted in Fig. 4.

Curves reported in Figs. 1 and 2 refer to situations still before failure, but all samples were eventually loaded until fracture occurred; they failed mainly at the contact region with the load platen. However, 13 samples failed within the gage region, thus revealing that brain tissue should be considered as a solid, neither a fluid nor a gel, exhibiting a fracture typical of a fibrous material (see the photo in Fig. 5). In particular, the nominal stress/stretch behaviour is reported in Fig. 5 (left), for a prismatic specimen loaded up to failure. It may be observed that the shape of the curve (after a path similar to that reported in Fig. 1, right) changes qualitatively, thus revealing the typical behaviour of a damaging material, in which the stress reaches a peak, followed by softening[4] (due to the progressive rupture of the filamentary structure of the material, see also Appendix B).

More precisely and with reference to Fig. 5, the curve can be divided into five parts: (1) an initial stiff response, followed by a (2) sort of "hardening behaviour", terminating into a (3) "locking behaviour" (marked in the detail of the figure) [in which the material exhibits a hardening higher than in (2)], which continues with a (4) hardening (marked in the detail of the figure) until a peak is reached and a (5) softening is evidenced

[4]With "softening" we denote here a negative tangent in the stress/stretch diagram.

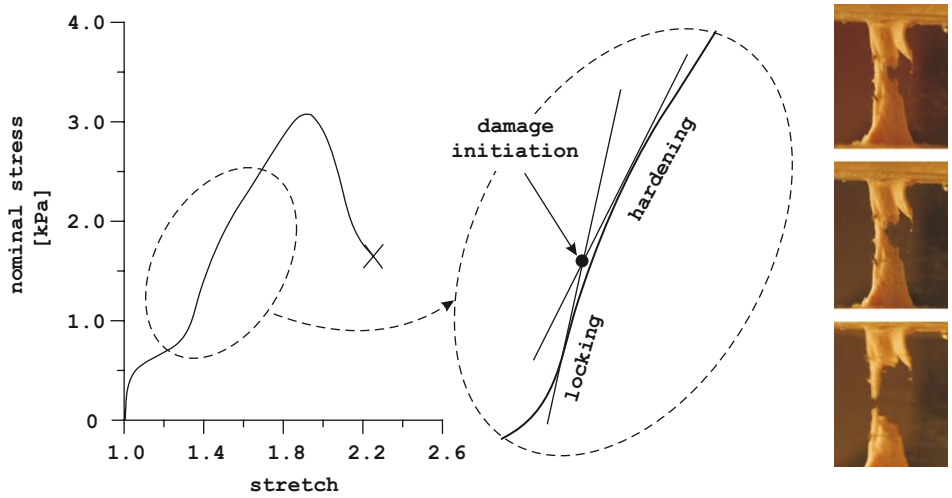

Fig. 5. The damage evolution and fracture process in a (14 mm/9.5 mm initial height/edge) prismatic specimen of white matter harvested from the occipital lobe in the frontal direction. Stress/stretch curve (left) and a photo sequence showing progressive fibrous damage occurring near the failure (right). The detail of the left figure is explicative of the employed conventional definition of damage initiation.

until separation occurs. Damage has been conventionally assumed to initiate when the "locking" branch of the curve in Fig. 5 degenerates into a "hardening" branch (see the detail of Fig. 5).[5] This has been found to occur at a stretch of 1.91 (mean value; range: $1.22 \div 2.68$; standard deviation: 0.42) and at nominal stress of 2.71 (mean value; range: $1.28 \div 7.1$; standard deviation: 1.47) kPa, while the peak of the stress/stretch curve was reached at a stretch of 2.39 (mean value; range: $1.92 \div 3.5$; standard deviation: 0.46) and stress of 3.43 (mean value; range: $1.55 \div 12.8$; standard deviation: 2.72) kPa. Final separation of the sample occurred at a stretch of 2.66 (mean value; range: $2.15 \div 3.8$; standard deviation: 0.49) and stress of 2.52 (mean value; range: $1.05 \div 9.4$; standard deviation: 2.19) kPa.

3. Uniaxial deformation at free drainage

In the pioneering work by Hakim et al. (1976) it was pointed out that brain parenchyma should be considered as a fluid-saturated porous material, so that a number of models have been developed, particularly for the analysis of the hydrocephalus, within the framework of (small or large strain) poroelasticity (Tada et al., 1994; Kaczmarek et al., 1997). However, the state-of-the-art is certainly not satisfactory. In fact:

- two-phase modelling is currently ignored by many authors and is sometimes criticized;
- only few, and indirect, evidences of poroelasticity are yet available. Some experimental evidence was given by Masserman (1934), who showed that a drainage of cerebrospinal

[5]The curvature transition separating locking and hardening type behaviours is a common indication of damage for a broad spectrum of fibrous materials, for instance, silicon carbide composite (Ishikawa et al., 1998) and scaffolds mimicking the extracellular matrix environment (Roeder et al., 2002).

fluid causes a reduction in ventricular size, continuing for 8 h, and by Miga et al. (2000), who measured certain displacements on an in vivo porcine experimental system, which were shown to agree with numerical simulations. The latter evidences are to be considered indirect since a non-poroelastic constitutive modelling could predict similar mechanical responses. An indisputable behaviour linked to the bi-phasic modelling is the volumetric shrinking of the brain due to the administration of hyperosmotic drugs such as mannitol (Bell et al., 1987) to alleviate elevated intracranial pressure or as a pre-surgical preparation. If there was no underpinning link relating the hydrated nature of the brain to its tissue matrix, the drug would not inhibit herniation;

- there is no agreement on the values of material parameters to be used. For instance, the drained volumetric compressibility suggested by Kaczmarek et al. (1997) on the basis of purely speculative arguments is much higher than that used by Tada et al. (1994);
- finally, if fundamental to explain deformation during hydrocephalus, why is interstitial fluid neglected in morphogenesis theories?

To clarify the situation, a uniaxial strain device has been designed and fabricated to test cylindrical specimens of brain tissue (5–8 mm/30 mm initial height/diameter) under free drainage at the top and bottom faces of the specimens (see Appendix C.1 for details). The device is in essence a miniaturised version of a so-called "oedometer" or "consolidometer", employed in geotechnical engineering (Taylor, 1948). This approach to testing has been employed for articular cartilage and heart muscle (Oloyede and Broom, 1991; Djerad et al., 1992), but never until now for brain tissues or other types of soft biological tissues. It provides the first *direct* evidence of poroelastic behaviour of brain parenchyma.

3.1. A comparison with the Terzaghi theory

As far as consolidation theory is concerned, the Terzaghi approach represents a particular case of the Biot general formulation (Biot, 1941) and is based on simplifying hypotheses, so that results depend only on one coefficient, the consolidation coefficient (Taylor, 1948, see Appendix C.2). By employing the Casagrande method (Holtz and Kovacs, 1981), we found this coefficient to be 0.37 (mean value; range: $0.01 \div 2.1$; standard deviation: 0.51) $\mathrm{mm}^2/\mathrm{min}$. A representative result of one of 12 tests is reported in Fig. 6, and compared with the predictions of Terzaghi consolidation theory for a consolidation coefficient $c_v = 0.45\,\mathrm{mm}^2/\mathrm{min}$. In the figure, the average consolidation ratio (current value of the specimen's shortening divided by the final shortening at the end of the consolidation) is reported after an initial step of 6 N load in a semi-logarithmic scale as a function of time (expressed in minutes) measured from the instant of the loading.

It should be noted that, although the consolidation coefficient is a material constant, a strong *size effect* is involved in the consolidation theory, so that the time needed to reach a certain level of consolidation in a problem scales with the square of the ratio between the drainage lengths involved in the problem under consideration and in the sample. For instance, if final consolidation was reached, say, in 100 min for the sample considered in Fig. 6 (in which the maximum drainage length is one half of the initial height, i.e. 6.9/2 mm) the same consolidation would be reached in 15 days for a drainage length of 5 cm, which can be involved in brain tissue deformation. This may shed some light on the time evolution of effects involved when brain parenchyma is deformed, with several possible implications [delayed effects may be important in hydrocephalus or, possibly, to

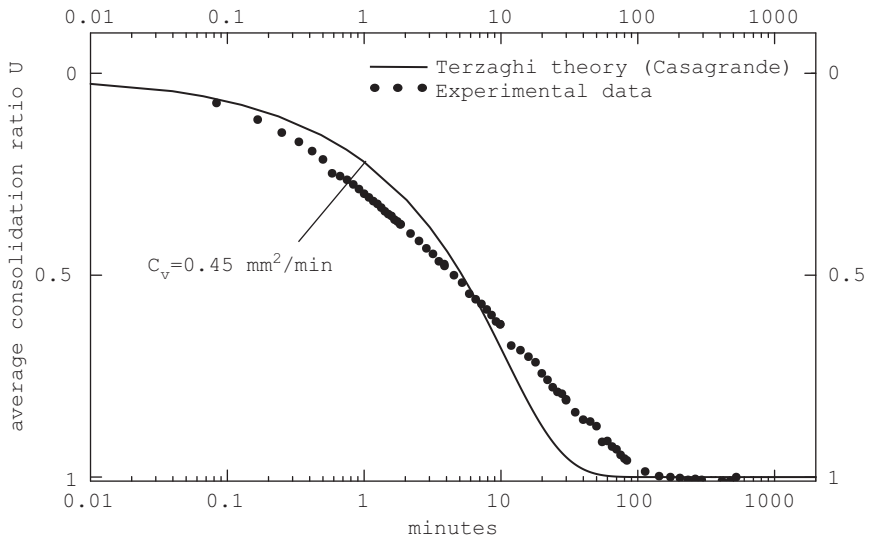

Fig. 6. Comparison between experimental data and Terzaghi consolidation theory: uniaxial tests on a cylindrical specimen (6.9 mm/30 mm initial height/diameter) harvested from the parietal lobe at free drainage at the upper and lower faces. The consolidation coefficient, denoted by c_v, is taken as 0.45 mm^2/min.

clarify the somewhat complex physiological alterations occurring during normal pressure hydrocephalus, where consolidation theory has been already advocated by Momjian et al. (2004)].

3.2. Is viscosity present in the solid phase?

A qualitative agreement with the Terzaghi consolidation theory can be deduced from Fig. 6 and from other results, reported in Appendix C.2. However, note that results may be more or less adherent to the theory. Deviations from the theoretical predictions may arise from different sources. First, homogeneities and geometrical tolerances of soft biological tissue samples are far from those inherent to engineering materials (e.g., soil samples). Second, results may be affected by post-mortem biochemical reactions which may slowly take place on the material. These factors may affect the results, seem to be inherent to the testing protocol, and appear difficult to quantify. Third, other deviations from the Terzaghi theory may come from:

- nonlinear behaviour of the material involved;
- nonlinear variation of porosity during the test;
- viscosity of the behaviour of the solid material.

As far as the first two are concerned, note that the strains which take place during the tests are small (mean value: 2.8%; range: 0.98% ÷ 5.53%; standard deviation: 1.26%). Hence, we think the first two points are not really important in our case, although under large

strains, which, for example, may occur during a cerebral edema or hydrocephalus, these nonlinearities could play a significant role.

In order to better understand the influence of the viscous deformation of the solid phase on the total deformation, we assume a viscoelastic behaviour instead of a purely elastic deformability of the solid phase, as advocated in the Terzaghi theory. Following Gibson and Lo (1961) (see also Christie, 1964), two constitutive parameters c_v and α appear in this model, which are described in more detail in Appendix C.3. The parameter c_v plays a similar role as that of the non-viscous case. By optimizing these two parameters through nonlinear least square fitting, we found an almost perfect agreement with the experimental data, see the dashed curve in Fig. 7 ($c_v = 2.74\,\mathrm{mm}^2/\mathrm{min}$ and $\alpha = 0.155$), where the same experimental data and the results for the Terzaghi model as in Fig. 6 are also reported.

The fitting of the experimental data with the Gibson and Lo theory gives $c_v = 2.07$ (mean value; range: $0.14 \div 6.18$; standard deviation: 1.81) $\mathrm{mm}^2/\mathrm{min}$ and $\alpha = 0.1$ (mean value; range: $0.03 \div 0.35$; standard deviation: 0.07).

In conclusion, we would like to mention that our results, although do not exclude (and even support) a viscous behaviour of the solid phase, clearly show that *the leading mechanism for delayed volumetric deformation is consolidation*.

3.3. A note on the consolidation theory and slow brain tissue deformation

Curves such as that reported in Fig. 6 are typical consolidation curves also exhibited by soft and fine soils. However, in contrast to these materials, the initial stiffness modulus under uniaxial deformation (so-called "drained, oedometric" in geotechnical engineering) is much higher than the initial unconfined modulus (with the term "initial", we denote the tangent stiffness modulus at zero stress) measured during tensile/compressive tests (Fig. 1). In particular, the measured mean values of these two quantities have been found to be 260 (mean value; range: $65 \div 555$; standard deviation: 130) kPa and 6.54 (mean value; range: $1.3 \div 15.64$; standard deviation: 4.69) kPa, respectively. Hence, the related ratio is 39.76, a value which supports the observation that brain tissue has a low volumetric compressibility

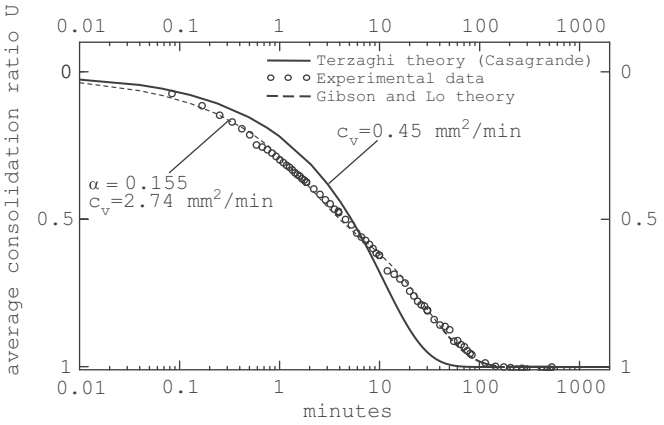

Fig. 7. Experimental data and numerical results according to the Terzaghi theory as for Fig. 6. The dashed curve indicates the prediction according to the Gibson and Lo theory.

even in drained conditions, which is again consistent with polymeric materials considered as nearly incompressible. Interpreted in terms of the linear theory of isotropic elasticity, the ratio corresponds to a value of initial, *drained* Poisson's ratio equal to[6] 0.496.

Due to the above-mentioned small drained volumetric compressibility, we point out that the uniaxial stress experiments (involving large deviatoric strains and described in the previous section) are not substantially influenced by the bi-phasic nature of brain parenchyma, so that drained and undrained behaviours do not differ much. To give more evidence to this important point, let us consider the initial values of the elastic parameters found for brain parenchyma. The initial *undrained* Poisson's ratio is 0.5 (corresponding to completely incompressible behaviour) and the *drained* value has been found equal to 0.496. Since volumetric deformability is not involved under shear, the ratio between the initial undrained and drained shear moduli is equal to unity. Therefore, the ratio of the initial undrained and drained elastic moduli results equal to $(1+0.5)/(1+0.496)=1.00267$, so that the two moduli are practically identical and uniaxial stress test becomes rather insensitive to the drainage conditions.

The above finding is important since it reconciles different approaches to mechanical modelling of brain parenchyma: due to the fact that volumetric drained compressibility is small when compared with the unconfined deformability, consolidation theory becomes dominant in problems that involve high values of mean stresses applied for a considerable time (as, for instance, during hydrocephalus or deformations accompanying slow cranial movements), while it plays the role of, say, a "correction" to a single phase nonlinear theory, when large deviatoric deformations occur (as, for instance, during convolutional development).

4. Conclusions

Brain tissues have been found to present distinctive mechanical properties, making them qualitatively similar to filled elastomers under cyclic uniaxial stress and to fine soils obeying consolidation theory under oedometric conditions. However, unlike soils and again similarly to elastomers, the ratio between initial oedometric modulus and initial elastic modulus is large. Our results suggest that mechanical modelling of brain tissue should involve a porosity model to account for the intrinsic porosity of the brain matter, at least in situations where substantial volumetric deformations are involved (during for instance hydrocephalus). Moreover, the drained behaviour of brain parenchyma should be treated as a nearly incompressible, nonlinear material, capable of permanent deformations and qualitatively similar to rubber-like materials. Although in the present paper we did not attempt to develop a constitutive model for the description of the mechanical behaviour of brain tissue under arbitrary deformations, we have shown that this model should reduce to the Terzaghi theory, when small deformations occur due to consolidation, and to a theory describing nearly incompressible rubber-like materials, when large deviatoric deformations are involved.

Acknowledgements

D.B. and G.F. gratefully acknowledge financial support from MURST-Cofin 2004, protocol no. 2004083253_002. The authors would also like to thank Marco Bragagna

[6]This value is in agreement with that documented by Kyriacou et al. (2002). Nearly incompressible behaviour is also suggested by Hakim et al. (1976).

(University of Trento), Gerhard Sommer and Christian Gasser (Graz University of Technology) for their helpful support during the experimental tests.

Appendix A. The research on brain tissue

A.1. A state-of-the-art on mechanical testing of brain tissue

Mechanical testing on human (and Rhesus monkey) brain tissues was initiated by Fallenstein et al. (1969) and Galford and McElhaney (1969, 1970). Cyclic shear tests have been performed by the former authors, while creep and relaxation experiments have been conducted under tension by the latter. Both these works refer to a small deformation range and are aimed to the understanding of dynamic properties, as related to traumatic brain injury [see the reviews by Hardy et al. (1994) and Goldsmith (2001)]. These pioneering works stimulated a continued research in which the brain parenchyma is assumed to be single-phase, incompressible and viscoelastic. In particular, oscillatory tests on porcine, bovine and rat brain specimens at small strain were performed by: Shuck and Advani (1972), proposing a failure criterion for brain tissue, Bilston et al. (1997) and Darvish and Crandall (2001), finding nonlinear effects already at, respectively, 0.1% and 1% strain, Arbogast and Margulies (1998), analyzing high frequency response, Thibault and Margulies (1998) and Gefen et al. (2003), determining some age-dependent changes in mechanical properties.

Large deformations, involving in particular uniaxial compression, were initiated by Estes and McElhaney (1970), who found the characteristic stress/strain curves concave upward for human and Rhesus monkey brain tissues. These experiments were followed by other investigations, mainly performed on porcine or bovine specimens and involving large strains, in particular, by Miller and Chinzei (1997), performing compressive stress/relaxation experiments and showing a strong dependence on strain rate, Donnelly and Medige (1997), presenting results which support nonlinear viscoelasticity, obtained with a single-pulse, high-strain-rate shear test on fresh human cadaver brain specimens, Bilston et al. (2001), reporting failure strains under large shear deformation, Prange and Margulies (2002), presenting results of shear and compression tests with stretches ranging between 0.5 and 1.6.

Miller et al. (2000) and Gefen and Margulies (2004) have compared in vivo and in vitro responses to mechanical tests on porcine brain tissue. The former authors have found (as already suggested by Metz et al., 1970) that in vivo and in vitro mechanical properties remain within the same order of magnitude, while the latter authors have reached an opposite conclusion.

A.2. Slow deformation of brain tissue calls for experimental investigation

It is crucial to observe from the above state-of-the-art that: (i) a linear (or sometime nonlinear) viscoelastic behaviour is always assumed to govern mechanical deformation of the brain tissue; (ii) a systematic investigation of large-strain, quasi-static, cyclic behaviour including damage and fracture of human brain tissue still does not exist; (iii) the effect of interstitial fluid has never been directly investigated and (iv) never discriminated from viscosity.

Hakim and co-workers present a series of data supporting a two-phase theory for brain parenchyma and emphasise the role of interstitial fluids on the mechanics of brain tissue during hydrocephalus (Hakim and Adams, 1965; Hakim and Burton, 1974; Hakim et al., 1976, 2001; Hakim and Hakim, 1984). We believe that there are many physiological instances pointing to biphasic representation. For instance, the effects of perfusion exhibited by Guillaume et al. (1997), the volumetric shrinking of the brain tissue following hyperosmotic drugs administration (such as mannitol, Bell et al., 1987; Schrot and Muizelaar, 2002), and the nature of cerebral edema itself show that the hydrated nature of brain parenchyma cannot be ignored. Surprisingly, no direct experimental evidence has been attempted to give evidence to the two-phasic nature of brain parenchyma.

Large and slow brain deformations are believed to play a crucial role during hydrocephalus, cerebral edema, convolutional development, and possibly in many other circumstances that may include robotic surgery and implantation. In geotechnical engineering, the understanding of the mechanical role of interstitial fluid in soils, which essentially follow the theories by Biot (1941) and Terzaghi (1943), generated a real scientific revolution (de Boer, 1999). Accordingly, the experimental investigation of the behaviour of brain tissue subject to slow and large deformations, with consideration of interstitial fluid, deserves appropriate attention.

Appendix B. Cyclic uniaxial loading tests

Uniaxial quasi-static cyclic tension/compression (or compression/tension) tests of prismatic or cylindrical specimens were performed on a computer-controlled, screw-driven high-precision tensile compressive testing machine (Messphysik, μ-Strain Instrument ME 30-1, Furstenfeld, Austria). The specimens were investigated in a perspex container filled with 0.9% physiological saline solution maintained at $37 \pm 0.1\,^{\circ}\mathrm{C}$ by a heater-circulation unit (type Ecoline E 200, Lauda; Lauda-Konigshofen, Germany) and the tensile compressive force was measured with a 25 N class 1 strain gage-load cell (model F1/25 N, AEP converter). For more details on the testing machine adapted for small biological specimens, see Holzapfel et al. (2004).

The upper and lower crossheads of the testing machine are moved in opposite directions so that the gage region of the samples is always in the same field of view. A crosshead stroke resolution of 0.04 μm and a minimum load resolution of 1 mN of the 25 N load cell is specified by the manufacturer. Digital control of the electric drive of the machine as well as data acquisition of the crosshead position and applied load were performed by an external digital controller (EDC 5/90 W, DOLI; Munich, Germany) especially designed for screw-driven tensile testing machines. Gage length and width were measured optically using a PC-based (CPU 586) videoextensometer (model ME 46-350, Messphysik) utilizing a full-image charge-coupled device (CCD) camera, that allows automatic gage mark and edge recognition (Holzapfel et al., 2004). The corresponding deformation data were averaged with respect to the measuring zone and sent to the data-processing unit in real time.

Experiments were conducted at a speed of 5 mm/min, corresponding to initial strain rates ranging between 5.5 and $9.3 \times 10^{-3}\,\mathrm{s}^{-1}$, on 86 prismatic and cylindrical samples. Dimension range of the specimens was 9–15 mm ÷ 5–11 mm initial height/diameter (or edge, for prismatic specimens), with aspect ratios lying in the interval 0.9–2.5 (Franceschini, 2006).

The specimens have been attached to the plexiglas loading platens of the testing machine using a commercial instant adhesive (Loctite®) and providing a small compression (corresponding to 1 mm relative displacement of the plates) for 20 s. Samples were taken at different locations and two different directions, along frontal and sagittal plane, as sketched in Fig. B.1.

Loading cycles have been performed up to various load levels, until large strain, damage and final failure of the specimen have been reached. In particular, initially cycles were imposed up to a maximum load of 0.03 N and, subsequently, the maximum loads to be reached were calibrated on the basis of the initial response. Typically, loading cycles were given at increments of 0.02 N, up to 0.12 N. At this loading level, the sample was monotonically loaded until failure.

Several results of cyclic behaviour before damage initiation are shown in the Figs. B.2–B.4 (additional data can be found in Franceschini, 2006), reported in terms of nominal stress (force divided by the initial cross-section area of the specimen), versus stretch (current specimen length divided by the initial length). Note that in all Figs. B.2–B.4 the first cycle is shown left (a) for the smallest loading step. Loading steps up to higher loads are considered in Figs. B.2 and B.3(b) and (c), and the complete cycles (evidencing pre-conditioning effects) relative to the loading step shown in (c) are reported in (d). Loading steps are reported in Fig. B.4(b) and (d), while the complete cycles (evidencing pre-conditioning effects) relative to the intermediate step (b) are reported in (c). These experimental results confirm the general trend shown in Figs. 1 and 2 and make evident the features previously commented, including the existence of permanent deformations.

The samples mainly failed at the contact region with the Plexiglas loading platens, but 13 failed within the gage region. These tests give evidence of the damage process and subsequent failure; results of three samples are presented in Fig. B.5 (additional data can be found in Franceschini, 2006).

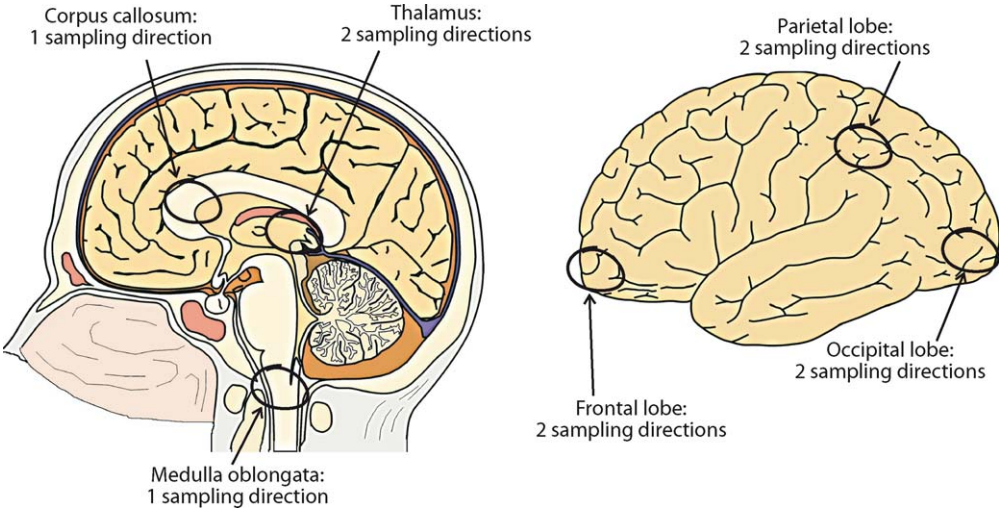

Fig. B.1. Specimen harvest locations.

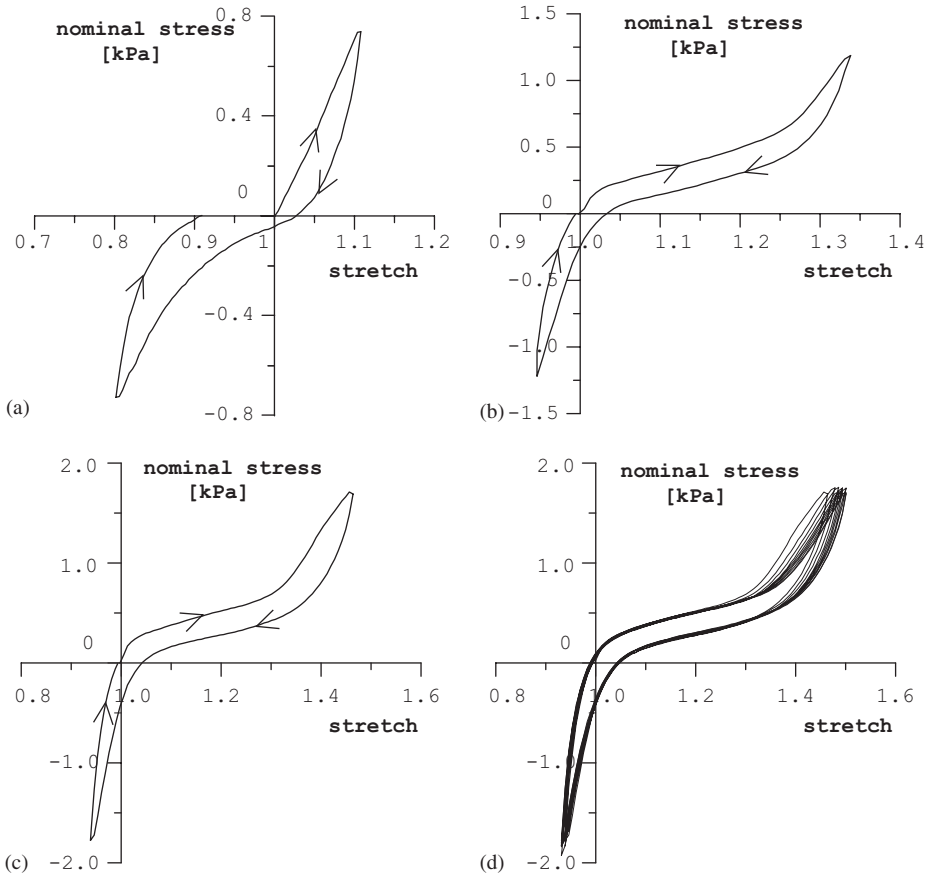

Fig. B.2. Cyclic behaviour of brain tissue to a stretch well below fracture, but approaching the damage threshold; nominal stress is reported versus stretch on a (13 mm/8.4 mm initial height/edge) prismatic specimen of white matter, harvested from the frontal lobe in the frontal direction. In (a)–(c), the first cycles of different loading steps (0.05 N, 0.08 N and 0.12 N) are reported, where arrows indicate the loading direction. Effect of preconditioning [for the load step (c) at 0.12 N of maximum load] becomes evident in (d), where 10 cycles have been performed.

Appendix C. Uniaxial deformation tests at free drainage and Terzaghi theory

C.1. The oedometric test

The recourse to a uniaxial strain apparatus with free drainage (so-called "oedometer" or "consolidometer" in geotechnical engineering, Taylor, 1948) is crucial to discriminate viscous behaviour from consolidation. This is indeed possible since the basic constituents of a brain specimen can be considered themselves incompressible (at least at the level of loading at which our experiments have been performed), therefore, if consolidation would not occur, the oedometric deformation would simply be zero.

An oedometer has been designed and fabricated (at the University of Trento, with the kind help of Mr. Marco Bragagna) for testing cylindrical specimens (30 mm/5–8 mm initial

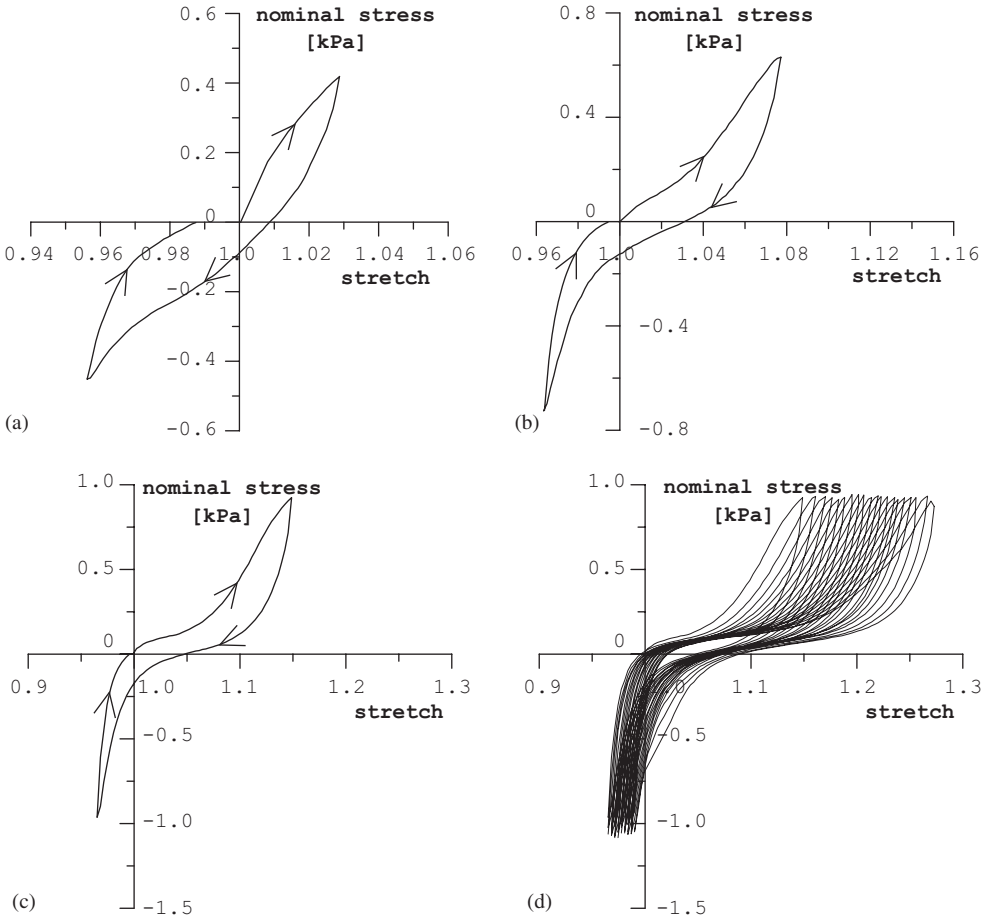

Fig. B.3. As in Fig. B.2, but results on a (10 mm/13 mm initial height/diameter) cylindrical specimen of white matter, harvested from the occipital lobe in the saggital direction. In (a)–(c), the first cycles of different loading steps (0.05, 0.08 and 0.12 N) are reported, where arrows indicate the loading direction. Effect of preconditioning [for the load step (c) at 0.12 N of maximum load] becomes evident in (d), where 20 cycles have been performed.

diameter/height) of brain parenchyma under free drainage at the top and bottom surfaces. A sketch of the device is reported in Fig. C.1 (see also Franceschini, 2006). It essentially consists of a metallic mould (all parts in contact with the samples are made of Inox AISI 304 steel) where the specimen is accommodated by hand and subsequently loaded through a cylindrical piston (made of polytetrafluoroethylens "PTFE", a material selected for its low weight, low friction coefficient, and chemical neutrality), subject to dead loading (through a loading frame made of Anticorodal aluminum). The contacts at the sample bottom and top are with a filter paper (Schleicher and Schuel no. 595, 110 mm diameter) against a porous metal [a commercial porous brass obtained through cold pressing and employed in geotechnical oedometers (from Controls S.r.l., Italy)], permitting free drainage of interstitial fluid. The tests have been performed under

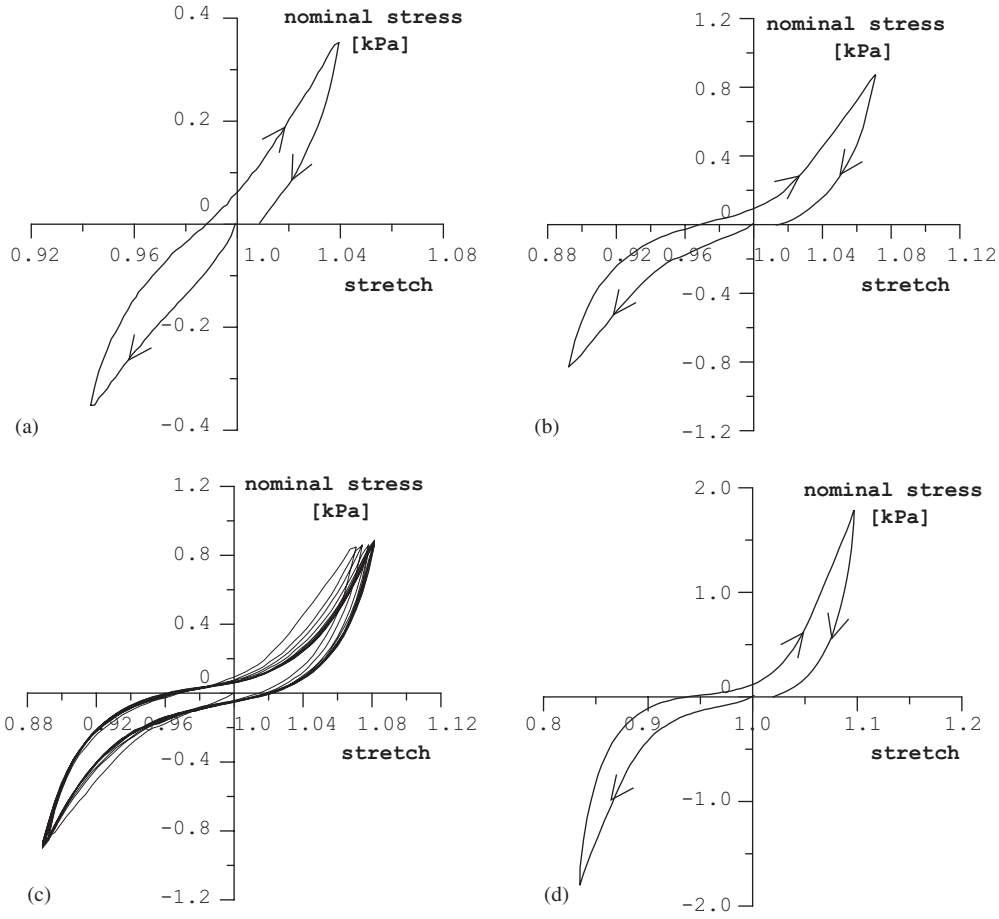

Fig. B.4. As in Fig. B.2, but results on a (18 mm/13.5 mm initial height/diameter) cylindrical specimen of white matter, harvested from the medulla oblongata. In (a), (b) and (d) the first cycles of different loading steps (0.05, 0.12 and 0.25 N) are reported, where arrows indicate the loading direction. Effect of preconditioning [for the load step (b) at 0.12 N of maximum load] becomes evident in (c), where 14 cycles have been performed.

physiological saline solution at room temperature (filling a cylindrical plastic container enclosing the device and thus preventing sample dehydration). Vertical displacement of the top of the sample was recorded employing an LVDT connected to an electronic acquisition system.

The dimensions of the device were dictated by the consideration of problems related to friction at the piston/die contact. Therefore, 12 samples have been harvested from the middle of the brain hemispheres, in the parietal lobe, a region selected in order to provide homogeneous specimens of the required dimensions. The specimens were excised using a trephine (see also Franceschini, 2006). The relatively large dimensions of our specimens precluded the investigation of possible anisotropy of fluid diffusion, which has been observed during acute cerebral ischemia by Green et al. (2002).

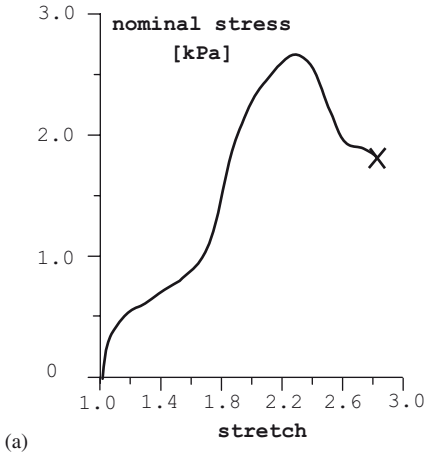

(a)

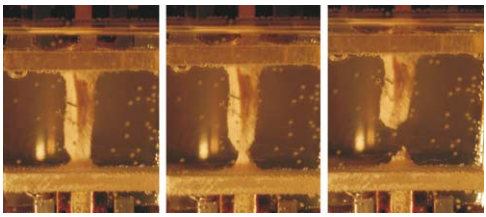

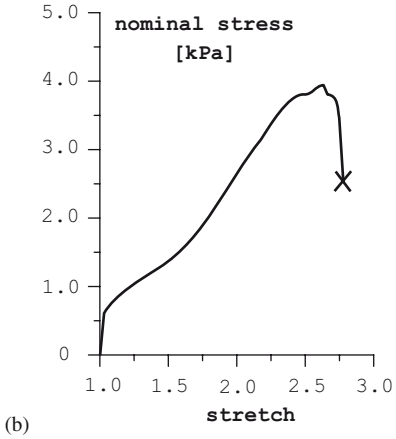

(b)

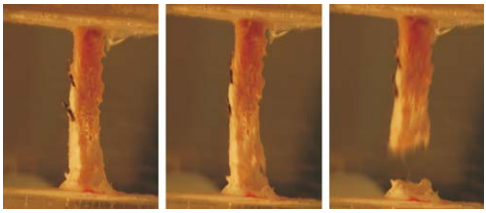

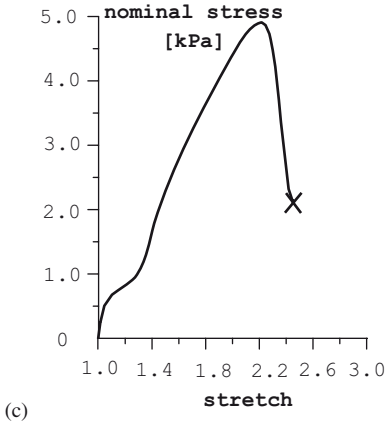

(c)

Fig. B.5. Damage evolution and fracture process in cylindrical and prismatic specimens of white and grey matter; nominal stress is reported versus stretch. The photos show the damage sequence leading to failure. Dimensions and sampling locations and directions are: 13 mm/8 mm (prismatic) white matter, parietal lobe, frontal direction (a); 15 mm/9.8 mm (cylindrical) gray matter, thalamus, saggital direction (b); 14 mm/8 mm (cylindrical) gray matter, thalamus, saggital direction (c).

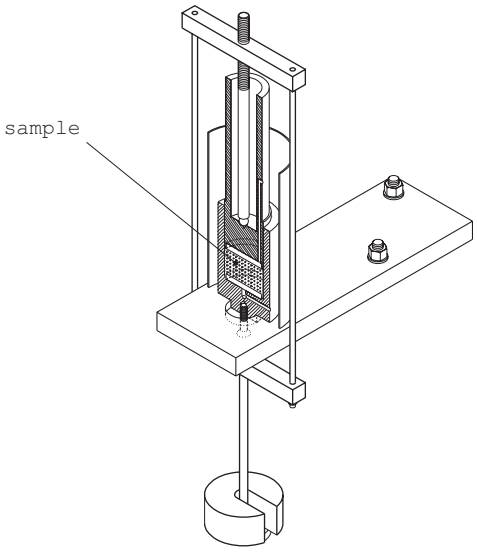

Fig. C.1. The uniaxial strain device permitting free drainage at the top and bottom of the sample.

The testing apparatus essentially permits the following two determinations:

(a) consolidation curve due to pore-pressure dissipation following a given load step;
(b) uniaxial strain (oedometric) compressibility obtained from a loading (or unloading) step sequence.

In the former test, vertical displacements are recorded versus time starting from the instant of a step loading application, until these "practically die out" (as will be explained later, graphs are generated with this test such as those shown in Figs. 3 and C.2–C.5). In the latter test, the strains at the end of consolidation occurring after various loading-steps are plotted versus the corresponding total applied stress, thus producing a "drained" uniaxial strain compressibility curve (examples of which are plotted in Fig. C.6).

One to four loading steps of 3 and 6 N were imposed in our tests (an intermediate step of 2 N has also been employed in one test). The loads were selected to be of the same order of magnitude as the pressures measured by Hakim et al. (1976) on two patients. One hour of time was expected after the set up of the test, before to assign the first loading. This time was checked to be sufficient to observe die out of displacements induced by apparatus self-load (the weight of the piston and loading frame is 1.3 N) and sample manipulation. Disturbances related to friction at the piston-die contact were considered unacceptable at loads smaller than 3 N for our apparatus.

Since the metallic mold is practically undeformable (at the prescribed load levels), the knowledge of the vertical displacement is directly linked to the measure of the uniaxial sample deformation, defined as the variation of the sample length divided by the initial length.

C.2. The Terzaghi theory

The average consolidation ratio U is defined as the ratio between the current value of the specimen's shortening and the final specimen's shortening at the end of consolidation, so

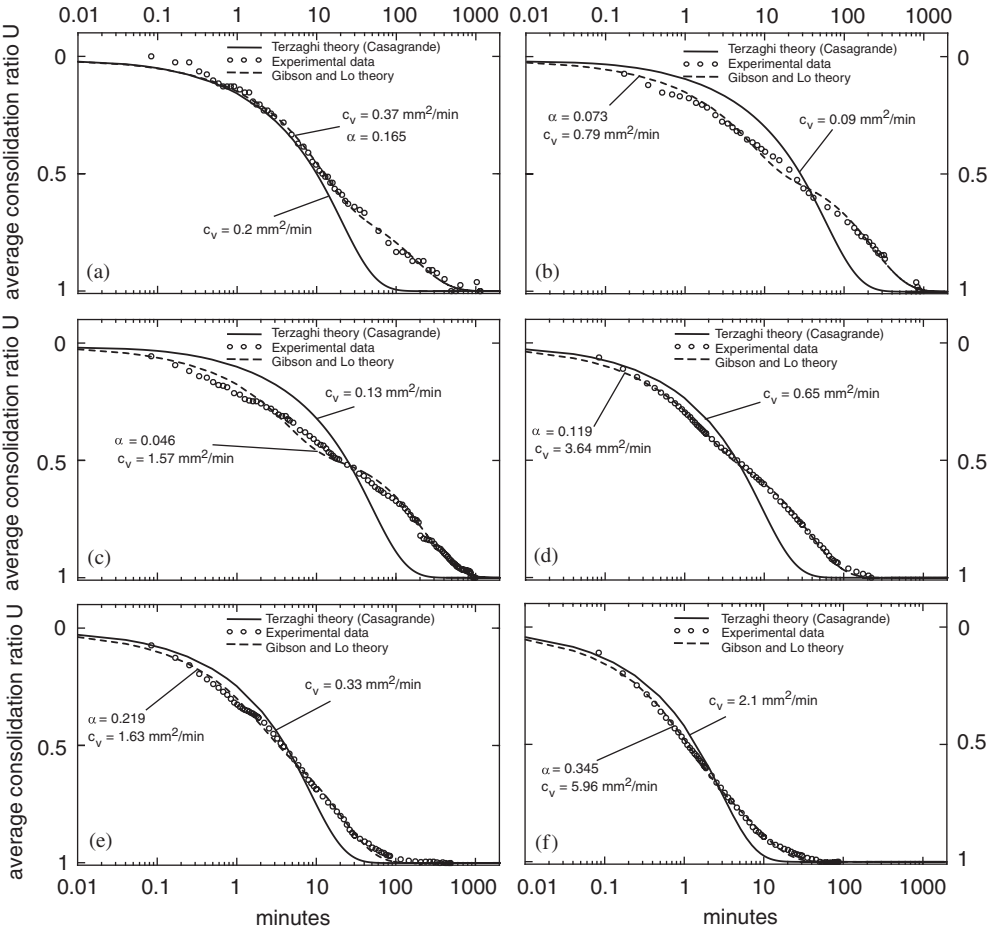

Fig. C.2. Comparison between experimental data, Terzaghi theory and Gibson and Lo theory for several uniaxial tests on cylindrical specimens under free drainage at the upper and lower faces. The Terzaghi consolidation coefficient c_v has been evaluated to be: 0.2 mm^2/min in (a); 0.09 mm^2/min in (b); 0.13 mm^2/min in (c); 0.65 mm^2/min in (d); 0.33 mm^2/min in (e) and 2.1 mm^2/min in (f). Results (a)–(e) were obtained at the first loading step of 3 N, while results (f) are obtained at the first loading step of 6 N.

that U ranges between 0 and 1. Test (a) permits plotting the evolution of the consolidation ratio versus time. This can be compared to the prediction of the Biot consolidation theory or its simpler version proposed by Terzaghi. We follow the Terzaghi theory—since we believe that evidence of consolidation should be sought with reference to the simplest possible theory—which is based on small-strain, linearly elastic behaviour of the porous material skeleton and the Darcy law of filtration. In the oedometric conditions the governing equation becomes

$$c_v \frac{\partial^2 p_w}{\partial z^2} = \frac{\partial p_w}{\partial t}, \tag{C.1}$$

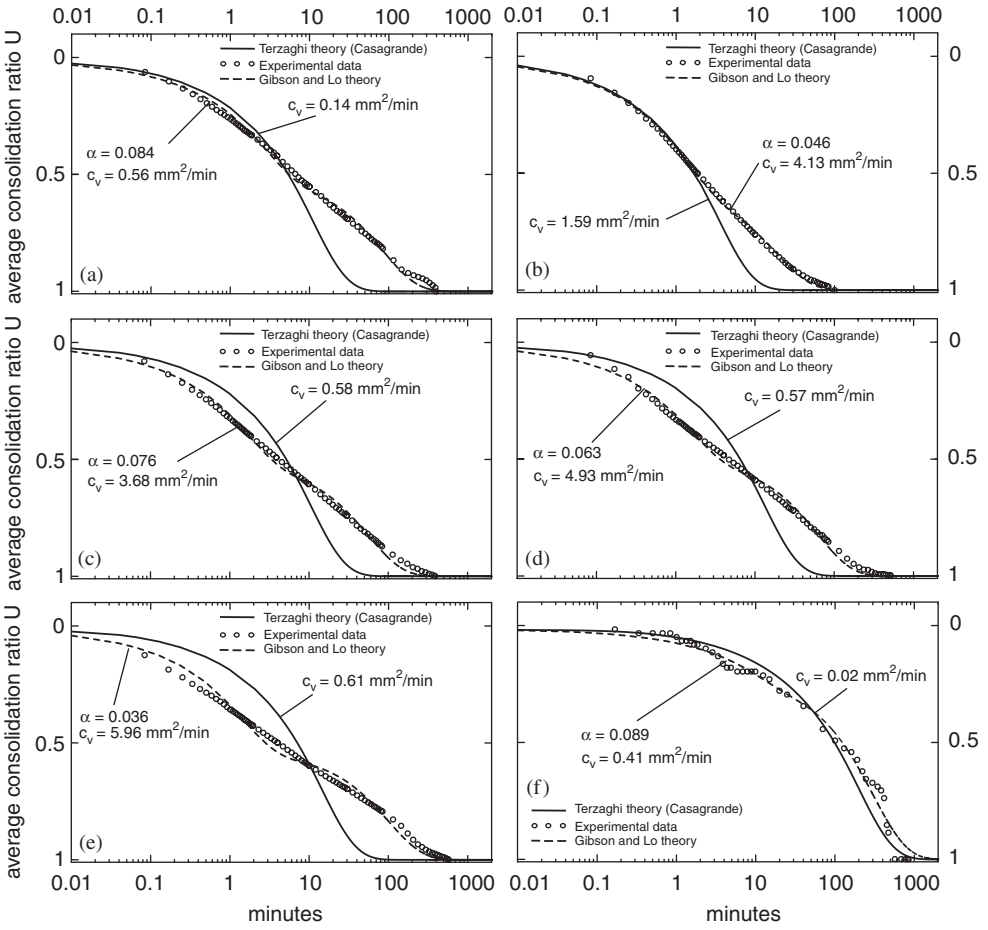

Fig. C.3. As in Fig. C.2, but the Terzaghi consolidation coefficient c_v has been evaluated to be: 0.14 mm^2/min in (a); 1.59 mm^2/min in (b); 0.58 mm^2/min in (c); 0.57 mm^2/min in (d); 0.61 mm^2/min in (e) and 0.02 mm^2/min in (f). Results in (a)–(e) were obtained at the first loading step of 6 N while results (f) are obtained at the second loading step of 3 N.

where z and t are the space and time variables, respectively, p_w is the pore fluid pressure, c_v is the coefficient of consolidation defined as

$$c_v = \frac{kM}{\gamma_w}, \tag{C.2}$$

in which k is the permeability, M is the elastic oedometric coefficient and γ_w is the specific weight of the saturating fluid.

The solution of Eq. (C.1), complemented with the initial and boundary conditions, respectively,

$$p_w(t=0) = p_{w0}, \quad p_w(z=0, z=2H) = 0, \tag{C.3}$$

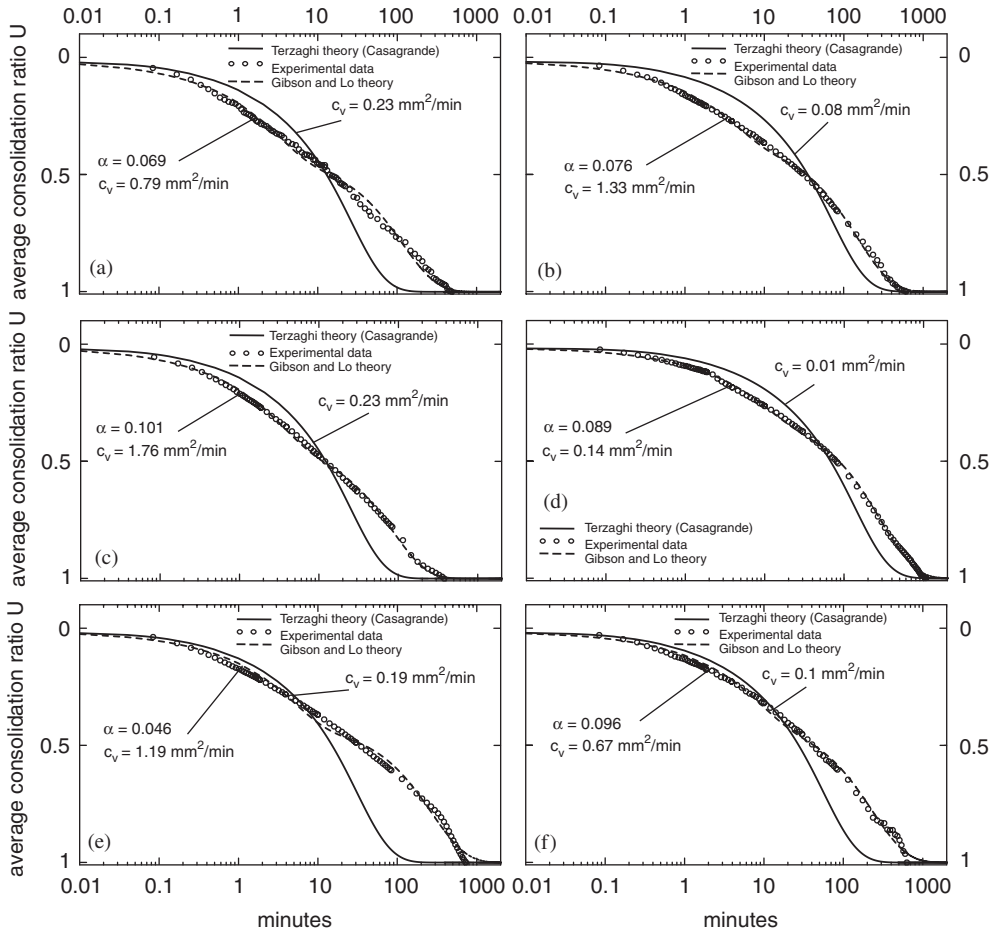

Fig. C.4. As in Fig. C.2, but the Terzaghi consolidation coefficient c_v has been evaluated to be: 0.23 mm^2/min in (a); 0.08 mm^2/min in (b); 0.23 mm^2/min in (c); 0.01 mm^2/min in (d); 0.19 mm^2/min in (e) and in 0.1 mm^2/min (f). Results (a)–(c) and (e) were obtained at the second loading step of 6 N, while results (d) at the second loading step of 3 N and (f) at the third loading step of 3 N.

corresponding to the oedometric test condition, is

$$p_{\mathrm{w}} = \sum_{m=0}^{\infty} \frac{4p_{\mathrm{w0}}}{\pi(2m+1)} \sin\frac{\pi(2m+1)}{2H} \exp[-(0.5\pi(2m+1))^2 T], \tag{C.4}$$

where H is the maximum drainage length (equal to 1/2 of the sample height in the oedometric test), p_{w0} is the initial (constant) value of pressure and

$$T = \frac{c_{\mathrm{v}} t}{H^2}. \tag{C.5}$$

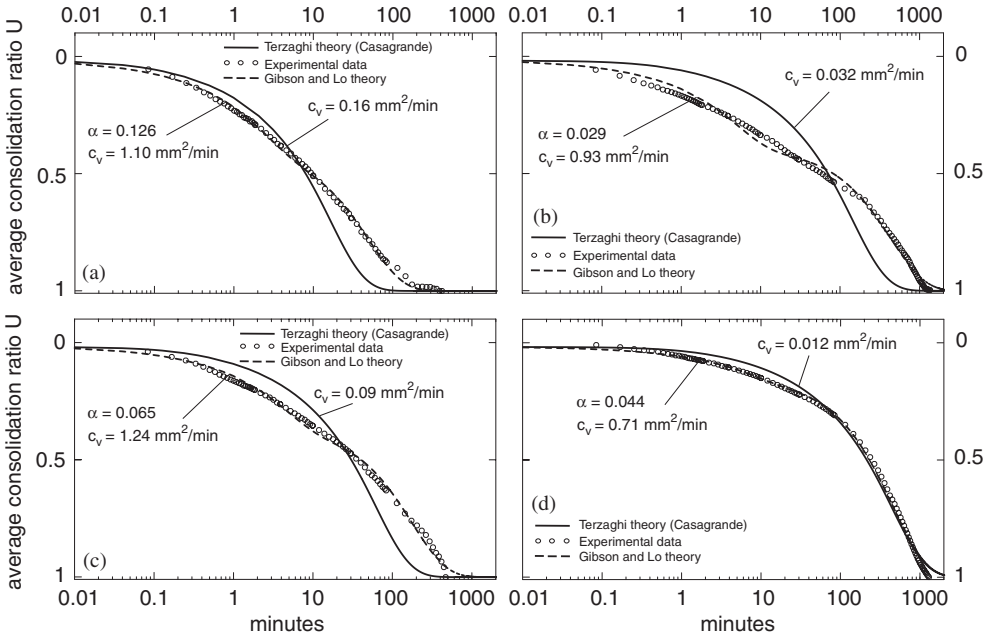

Fig. C.5. As in Fig. C.2, but the Terzaghi consolidation coefficient, c_v, has been evaluated to be: 0.16 mm^2/min in (a); 0.032 mm^2/min in (b); 0.09 mm^2/min in (c) and 0.012 mm^2/min in (d). Results (a)–(b) were obtained at the third loading step of 6 N, results (c) at the third loading step of 3 N and results (d) at the fourth loading step of 2 N.

Employing a linear constitutive relation for the elastic porous material and introducing the following definition of the consolidation ratio

$$U_z = 1 - \frac{p_w}{p_{w0}}, \tag{C.6}$$

which represents the current value of the specimen's shortening at coordinate z divided by the final shortening at the end of the consolidation, Eq. (C.4) becomes

$$U_z = 1 - \sum_{m=0}^{\infty} \frac{4}{\pi(2m+1)} \sin\frac{\pi(2m+1)}{2H} \exp[-(0.5\pi(2m+1))^2 T]. \tag{C.7}$$

Note that the consolidation ratio (C.7) is a function of the space and time variables z and t, of the consolidation coefficient c_v and sample height $2H$. Accordingly to the definition previously given, the average consolidation ratio results as the average of U_z over the height of the sample, namely

$$U = 1 - \sum_{m=0}^{\infty} \frac{8}{\pi^2(2m+1)^2} \exp[-(0.5\pi(2m+1))^2 T], \tag{C.8}$$

therefore, the Terzaghi theory predicts, for a given drainage length H, that the average consolidation ratio U is a function of time and of the coefficient of consolidation c_v.

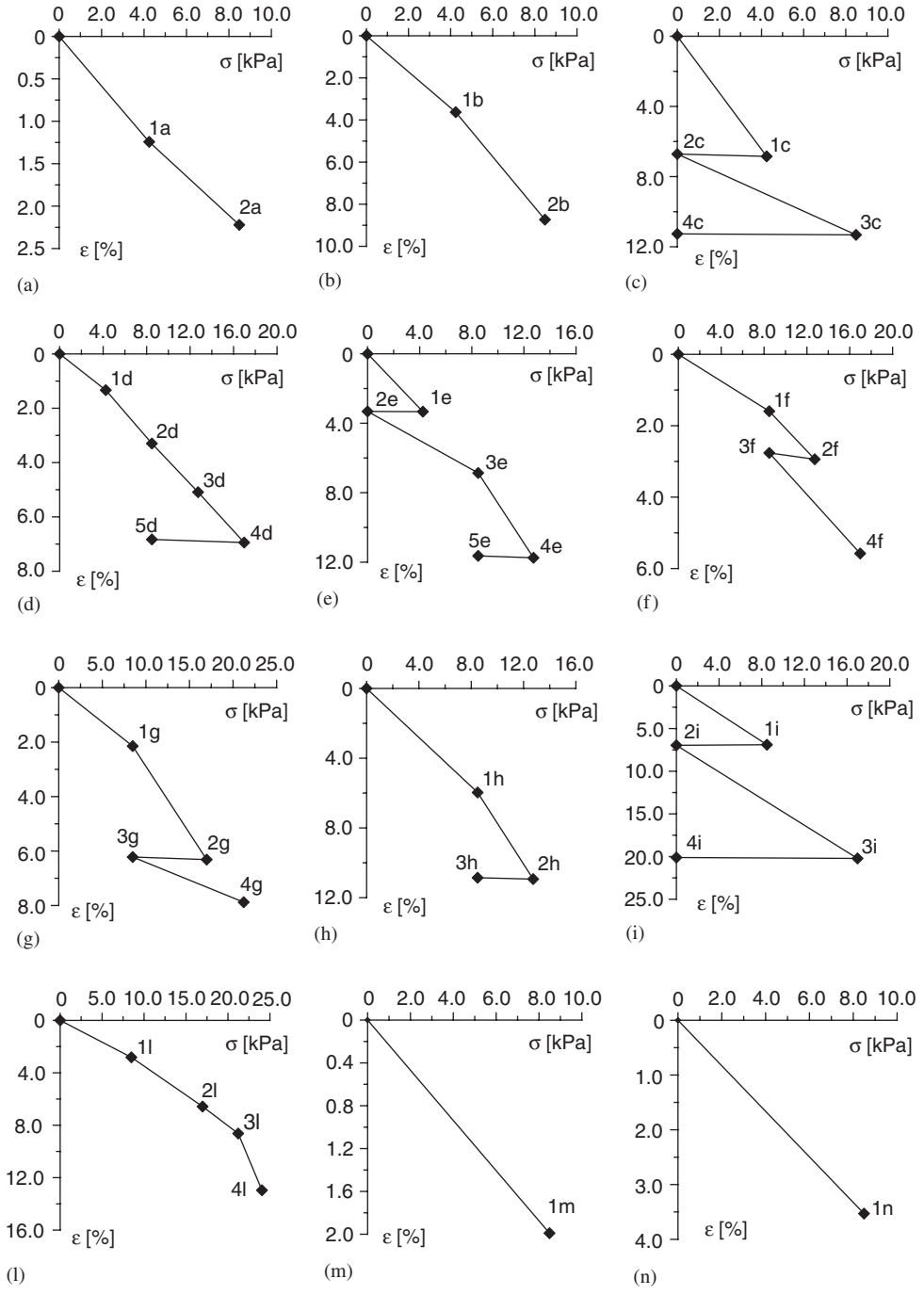

Fig. C.6. Engineering strain ε (in percent) versus stress σ, evidencing the drained oedometric compressibility of brain parenchyma. Only loading steps have been imposed in (a), (b), (l), (m) and (n) in particular, one loading step in (m) and (n), two loading steps in (a) and (b) and four in (l). One unloading step has been imposed in (d), (f), (h) and (g), and two in (c), (e) and (i).

It follows that a test of the type (a) may be used to evaluate c_v. This evaluation is, however, not immediate; it is in fact well-known in geotechnical engineering that when a load step is applied to an oedometer, an immediate displacement occurs, which cannot be related to the Terzaghi theory. This is believed to be only minimal due to the instantaneous deformation of the sample, but mainly related to "spurious effects", such as closure of possible gaps at the sample/piston contact and movements of the measurement system. Therefore, two methods are accepted in geotechnical engineering to eliminate this displacement from the results: the Taylor and the Casagrande methods (Holtz and Kovacs, 1981). We have followed the latter and our results are shown in Figs. 6 and C.2–C.5, in terms of the average consolidation ratio U, Eq. (C.8), versus time (additional data can be found in Franceschini, 2006). In the figures, also predictions of Gibson and Lo's theory (to be introduced later) are included (dashed).

Note that the initial oedometric modulus M appearing in Eq. (C.2) has been calculated from our data to be 260 (mean value; range: $65 \div 555$; standard deviation: 130) kPa. This value yields through Eq. (C.2) a mean initial permeability k equal to 2.42×10^{-10} (mean value; range: $6.15 \times 10^{-12} \div 1.58 \times 10^{-9}$; standard deviation: 3.47×10^{-10}) m/s.

It should be noted that the consolidation curves reported in Figs. 6 and C.2–C.5 have been obtained in correspondence of the loading steps, reported in terms of drained compressibility curves (stress versus strain at the end of consolidation for different loading/unloading steps) in Fig. C.6. The correspondence between the loading steps reported in Figs. C.6 and Figs. 6 and C.2–C.5 is indicated in Table 1.

Table 1
Correspondence between consolidation curves reported in Figs. 6 and C.2–C.5 and drained oedometric compressibility curves reported in Fig. C.6

Loading step in Fig. C.6	Correspondence in Figs. 6 and C.2–C.5	Loading step (N)
1(a)	C.2(a)	3
2(a)	C.3(f)	3
1(b)	C.2(b)	3
1(c)	C.2(c)	3
3(c)	C.4(a)	6
1(d)	C.2(d)	3
2(d)	C.4(b)	6
3(d)	C.4(f)	3
1(e)	C.2(e)	3
3(e)	C.5(a)	6
1(f)	6	6
1(g)	C.2(f)	6
2(g)	C.4(c)	6
1(h)	C.3(a)	6
2(h)	C.4(d)	3
1(i)	C.3(b)	6
3(i)	C.5(b)	12
1(l)	C.3(c)	6
2(l)	C.4(e)	6
3(l)	C.5(c)	3
4(l)	C.5(d)	2
1(m)	C.3(d)	6
1(n)	C.3(e)	6

C.3. A viscous correction to the Terzaghi theory

Gibson and Lo (1961) accepted the general assumptions of the Terzaghi theory, but introduced a rheological model consisting of a Hookean spring in series with a Kelvin body. The total strain ε due to an effective stress increment $p(t)$ at time t can be written as the sum of two contributions:

$$\varepsilon = p(t)/E_1 + \varepsilon_2, \tag{C.9}$$

where E_1 is the elastic modulus of the Hookean spring and ε_2 is the strain of the Kelvin body, characterized by the elastic modulus E_2 and the viscosity η, so that

$$p(t) = E_2\varepsilon_2 + \eta\dot{\varepsilon}_2. \tag{C.10}$$

By solving expression (C.10) for ε_2, substituting into Eq. (C.9), and inserting the result into the basic equation of consolidation, we get an equation that can be solved for p_w. Therefore, the general solution with the boundary and initial conditions (C.3) in terms of the average consolidation ratio becomes

$$U = 1 + \frac{8}{\pi^2}\sum_{n=0}^{\infty}\frac{1}{(n+1)^2}\left[\left\{\frac{(n+1)^2\pi^2/E_*) - x_1}{x_1 - x_2}\right\}e^{-x_2 T/4} - \left\{\frac{(n+1)^2\pi^2/E_*) - x_2}{x_1 - x_2}\right\}e^{-x_1 T/4}\right], \tag{C.11}$$

where

$$x_1 = 0.5\left[4E_*\alpha + (n+1)^2\pi^2 + \sqrt{(4E_*\alpha + (n+1)^2\pi^2)^2 - 16\alpha(n+1)^2\pi^2}\right], \tag{C.12}$$

$$x_2 = 0.5\left[4E_*\alpha + (n+1)^2\pi^2 - \sqrt{(4E_*\alpha + (n+1)^2\pi^2)^2 - 16\alpha(n+1)^2\pi^2}\right], \tag{C.13}$$

$$E_* = \frac{E_1 + E_2}{E_2}, \quad \alpha = \frac{E_2 H^2}{\eta c_v}, \quad T = \frac{c_v t}{H^2}, \quad c_v = \frac{kE_1}{\gamma_w}.$$

Results reported in Figs. 7 and C.2–C.5 with the dashed curves have been obtained by optmizing c_v and the viscous parameter α through a nonlinear least squares method (function FindFit, available in Mathematica® 5.0.1).

References

Arbogast, K.B., Margulies, S.S., 1998. Material characterization of the brainstem from oscillatory shear tests. J. Biomech. 31, 801–807.

Bell, B.A., Smith, M.A., Kean, D.M., McGhee, C.N., MacDonald, H.L., Miller, J.D., Barnett, G.H., Tocher, J.L., Douglas, R.H., Best, J.J., 1987. Brain water measured by magnetic resonance imaging. Correlation with direct estimation and changes after mannitol and dexamethasone. Lancet 1, 66–69.

Bilston, L.E., Liu, Z.Z., Nhan, P.T., 1997. Linear viscoelastic properties of bovine brain tissue in shear. Biorheology 34, 377–385.

Bilston, L.E., Liu, Z.Z., Phan-Thien, N., 2001. Large strain behaviour of brain tissue in shear: some experimental data and differential constitutive model. Biorheology 38, 335–345.

Biot, M.A., 1941. General theory of three-dimensional consolidation. J. Appl. Phys. 12, 155–164.

de Boer, R., 1999. Theory of Porous Media. Springer, Berlin, Heidelberg, New York.

Burland, J.B., Jamiolkowshi, M., Viggiani, C., 2003. The stabilisation of the leaning tower of Pisa. Soil Found. 43, 63–80.

Christie, I.F., 1964. A re-appraisal of Merchant's contribution to the theory of consolidation. Geotechnique 14, 309–320.
Cluzel, P., Lebrun, A., Heller, C., Lavery, R., Viovy, J.L., Chatenay, D., Caron, F., 1996. DNA: An extensible molecule. Science 271, 792–794.
Darvish, K.K., Crandall, J.R., 2001. Strain conditioning in the dynamic viscoelastic response of brain tissue. BED-Vol. 50, Bioengineering Conference ASME 2001, pp. 893–894.
Dingwall, E.J., 1931. Artificial Cranial Deformation: A Contribution to the Study of the Ethnic Mutilations. John Bale, Sons and Danielsson, London.
Djerad, S.E., Duburck, F., Naili, S., Oddou, C., 1992. Analysis of the unsteady rheological behaviour of a sample from cardiac muscle. Comptes Rendus de L' Academie des Science serie II 315, 1615–1621.
Donnelly, B.R., Medige, J., 1997. Shear properties of human brain tissue. J. Biomech. Eng. 119, 423–432.
Dorfmann, A., Ogden, R.W., 2004. A constitutive model for the Mullins effect with permanent set in particle—reinforced rubber. Int. J. Solids Struct. 41, 1855–1878.
Estes, M.S., McElhaney, J.H., 1970. Response of brain tissue of compressive loading. ASME 70-BHF-13, 1–4.
Fallenstein, G.T., Hulce, V.D., Melvin, J.W., 1969. Dynamic mechanical properties of human brain tissue. J. Biomech. 2, 217–226.
Franceschini, G., 2006. The mechanics of human brain tissue. Ph.D. Thesis, University of Trento, available online at www.ing.unitn.it/~francesg/.
Galford, J.E., McElhaney, J.H., 1969. Some viscoelastic properties of scalp, brain and dura. ASME 69-BHF-7, 1–8.
Galford, J.F., McElhaney, J.H., 1970. A viscoelastic study of scalp, brain and dura. J. Biomech. 3, 211–221.
Gefen, A., Gefen, N., Zhu, Q.L., Raghupathi, R., Margulies, S.S., 2003. Age-dependent changes in material properties of the brain and braincase of the rat. J. Neurotrauma 20, 1163–1177.
Gefen, A., Margulies, S.S., 2004. Are in vivo and in situ brain tissues mechanically similar? J. Biomech. 37, 1339–1352.
Gibson, R.E., Lo, K.Y., 1961. A theory of consolidation for soils exhibiting secondary compression. Acta Polytech. Scand. Ci 10, 1–15.
Goldsmith, W., 2001. The state of head injury biomechanics: past, present, and future: part 1. Crit. Rev. Biomed. Eng. 29, 441–600.
Green, H.A.L., Pena, A., Price, C.J., Warburton, E.A., Pickard, J.D., Carpenter, T.A., Gillard, J.H., 2002. Increased anisotropy in acute stroke—a possible explanation. Stroke 33, 1517–1521.
Guillaume, A., Osmont, D., Gaffie, D., Sarron, J.C., Quandieu, P., 1997. Effects of perfusion on the mechanical behavior of the brain exposed to hypergravity. J. Biomech. 30, 383–389.
Hakim, S., Adams, R.D., 1965. The special clinical problem of symptomatic hydrocephalus with normal cerebrospinal fluid pressure. Observations on cerebrospinal fluid hydrodynamics. J. Neurol. Sci. 2, 307–327.
Hakim, S., Burton, J.D., 1974. The engineering of hydraulic valves for the treatment of hydrocephalus. Eng. Med. 3, 3–7.
Hakim, S., Hakim, C., 1984. A biomechanical model of hydrocephalus and its relationship to treatment. In: Shapiro, K., Marmarou, A., Portnoy, H. (Eds.), Hydrocephalus. Raven Press, New York, pp. 143–160.
Hakim, C.A., Hakim, R., Hakim, S., 2001. Normal-pressure hydrocephalus. Neurosurg. Clin. N. Am. 36, 761–773.
Hakim, S., Venegas, J.G., Burton, J.D., 1976. The physics of the cranial cavity, Hydrocephalus and normal pressure. hydrocephalus: Mechanical interpretation and mathematical model. Surg. Neurol. 5, 187–210.
Hardy, W.N., Khalil, T.B., King, A.I., 1994. Literature-review of head-injury biomechanics. Int. J. Impact Eng. 15, 561–586.
Holtz, R.D., Kovacs, W.D., 1981. An Introduction to Geotechnical Engineering. Prentice Hall, Inc., Englewood Cliffs, NJ.
Holzapfel, G.A., Sommer, G., Regitnig, P., 2004. Anisotropic mechanical properties of tissue components in human atherosclerotic plaques. J. Biomech. Eng. 126, 657–665.
Hourwink, R., 1958. Elasticity, Plasticity and Structure of Matter. Dover Publication Inc.
Hutchison, B.L., Hutchison, L.A.D., Thompson, J.M.D., Mitchell, E.A., 2004. Plagiocephaly and brachycephaly in the first two years of life: A prospective cohort study. Pediatrics 114, 970–980.
Ishikawa, T., Kajii, S., Matsunaga, K., Hogami, T., Kohtoku, Y., Nagasawa, T., 1998. A tough, thermally conductive silicon carbide composite with high strength up to 1600 °C in air. Science 282, 1295–1297.
Kaczmarek, M., Subramaniam, R.P., Neff, S.R., 1997. The hydromechanics of hydrocephalus: Steady-state solutions for cylindrical geometry. Bull. Math. Biol. 59, 295–323.

Kingsbury, M.A., Rehen, S.K., Contos, J.J.A., Higgins, C.M., Chun, J., 2003. Non-proliferative effects of lysophosphatidic acid enhance cortical growth and folding. Nat. Neurosci. 6, 1292–1299.

Kyriacou, S.K., Mohamed, A., Miller, K., Neff, S., 2002. Brain mechanics for neurosurgery: modelling issues. Biomech. Model Mechanobiol. 1, 151–164.

Lewin, R., 1980. Is your brain really necessary? Science 210, 1232–1234.

Lion, A., 1997. On the large deformation behaviour of reinforced rubber at different temperatures. J. Mech. Phys. Solids 45, 1805–1834.

Masserman, J.H., 1934. Cerebrospinal hydrodynamics: IV. Clinical experimental studies. Arch. Neurol. Psychiat. 32, 523–553.

Metz, H., McElhaney, J., Ommaya, A.K., 1970. A comparison of the elasticity of live, dead, and fixed brain tissue. J. Biomech. 3, 453–458.

Miga, M.I., Paulsen, K.D., Hoopes, P.J., Kennedy, F.E., Hartov, A., Roberts, D.W., 2000. In vivo modeling of interstitial pressure in the brain under surgical load using finite elements. J. Biomech. Eng. 122, 354–363.

Miller, K., Chinzei, K., 1997. Constitutive modelling of brain tissue: Experiment and theory. J. Biomech. 30, 1115–1121.

Miller, K., Chinzei, K., 2002. Mechanical properties of brain tissue in tension. J. Biomech. 35, 483–490.

Miller, K., Chinzei, K., Orssengo, G., Bednarz, P., 2000. Mechanical properties of brain tissue in vivo: Experiment and computer simulation. J. Biomech. 33, 1369–1376.

Momjian, S., Owler, B.K., Czosnyka, Z., Czosnyka, M., Pena, A., Pickard, J.D., 2004. Pattern of white matter regional cerebral blood flow and autoregulation in normal pressure hydrocephalus. Brain 127, 965–972.

Mullins, L., 1947. Effect of stretching on the properties of rubber. J. Rubber Res. 16, 275–289.

Ogden, R.W., 1972. Large deformation isotropic elasticity—on the correlation of theory and experiment for incompressible rubberlike solids. Proc. R. Soc. Lond. A 326, 565–584.

Ogden, R.W., 1986. Recent advances in the phenomenological theory of rubber elasticity. Rubber Chem. Technol. 59, 361–383.

Ogden, R.W., Roxburgh, D.G., 1999. A pseudo-elastic model for the Mullins effect in filled rubber. Proc. R. Soc. Lond. A 455, 2861–2878.

Oloyede, A., Broom, N.D., 1991. Is classical consolidation theory applicable to articular cartilage deformation? Clin. Biomech. 6, 206–212.

Prange, M.T., Margulies, S.S., 2002. Regional, directional, and age-dependent properties of the brain undergoing large deformation. J. Biomech. Eng. 124, 244–252.

Richman, D.P., Steward, R.M., Hutchinson, J.W., Caviness Jr., V.S., 1975. Mechanical model of brain convolutional development. Science 189, 18–21.

Roeder, B.A., Kokini, K., Sturgis, J.E., Robinson, J.P., Voytik-Harbin, S.L., 2002. Tensile mechanical properties of three-dimensional type I collagen extracellular matrices with varied microstructure. J. Biomech. Eng. 124, 214–222.

Scannell, J.W., 1997. Determining cortical landscapes. Nature 386, 452.

Schrot, R.J., Muizelaar, J.P., 2002. Mannitol in acute traumatic brain injury. Lancet 359, 1633–1634.

Shuck, L.Z., Advani, S.H., 1972. Rheological response of human brain tissue in shear. J. Basic Eng. 94, 905–911.

Storm, C., Pastore, J.J., MacKintosh, F.C., Lubensky, T.C., Janmey, P.A., 2005. Nonlinear elasticity in biological gels. Nature 435, 191–194.

Tada, Y., Nagashima, T., Takada, M., 1994. Biomechanics of brain tissue (simulation of cerebrospinal-fluid flow). JMSE Int. J. 37, 188–194.

Taylor, D.W., 1948. Fundamentals of Soil Mechanics. Wiley, New York.

Terzaghi, K., 1943. Theoretical Soil Mechanics. Wiley, New York.

Thibault, K.L., Margulies, S.S., 1998. Age-dependent material properties of head porcine cerebrum: Effect on pediatric inertial head injury criteria. J. Biomech. 31, 1119–1126.

Twizell, E.H., Ogden, R.W., 1983. Non-linear optimization of the material constants in Ogden's stress-deformation function for incompressible isotropic elastic materials. J. Austral. Math. Soc. Ser. B 24, 424–434.

Van Essen, D.C., 1997. A tension-based theory of morphogenesis and compact wiring in the central nervous system. Nature 385, 313–318.